Phase Analysis Studies of Titanium–Chromium Oxides Derived from Rutile by Crystallographic Shear

D. K. PHILP* AND L. A. BURSILL†

School of Chemistry, University of Western Australia, Nedlands 6009, Australia

An electron microscopic phase analysis of rutile plus 0–25 mole% $CrO_{1.5}$, at 1573°K, is reported. A "rutile" matrix, containing mottled contrast, short crystallographic shear (CS) planes and an unusually high density of dislocations, coexists with lamellae of (253)$_r$ CS planes (approx $MX_{1.97}$) for 0–8 mole% $CrO_{1.5}$. For 8–25 mole% at least 50 different structures were characterized. Within experimental error there is an essentially continuous variation of CS plane orientation and spacing with composition. The CS planes cooperatively reorient from (253)$_r$ to (121)$_r$, pivoting about the [1$\bar{1}$1]$_r$ zone axis. The CS plane spacing simultaneously decreases from 2.4 to 1.3 nm. Lattice images show that both the spacing and orientation of the CS planes are very uniform within each crystal flake, confirming our earlier suggestion of *continuous ordered* solid solution. The results are compared to previous studies of chromia-doped rutile and other reduced rutile systems.

1. Introduction

Evidence for the existence of a large number of rutile-derived CS structures has already been presented (*1*). They conform to the general formula M_nO_{2n-p}, with $4 \leqslant n \leqslant \infty$, $1 \leqslant p \leqslant \infty$, n and p integral and M = Ti or (Ti,Cr). They fall into families with different CS planes

$$(hkl)_r = p \cdot (121)_r + q \cdot (011)_r,^1$$

(q also integral). The different members of a family have different CS plane spacings D_{sp}. In principle, a continuous sequence of ordered structures may be produced by varying the proportions (i) of (121)$_r$ and (011)$_r$ segments along the CS plane and/or (ii) of two members of one family normal to the CS plane. The general structural principles, and observations of texture, reaction mechanisms, and thermodynamics were reviewed in Reference (*2*).

* Present address: Defence Standards Laboratories, P.O. Box 50, Ascot Vale 3032, Australia.

† Present address: Department of Physics, University of Melbourne, Parkville, 3052, Australia.

¹ Subscript r denotes indices referred to the rutile cell or subcell.

We now report the results of a detailed phase analysis study using electron diffraction, of the system rutile plus 0–25 mole% $CrO_{1.5}$, mainly at 1573°K, and mainly from reference (*3*). The aims were, as far as possible, (*a*) to find the precise sequence of p, q, and D_{sp} values as a function of composition at one temperature and (*b*) to examine the limitations of the model for *continuous ordered* "solid solution." What is the equilibrium situation? What variations in spacing and orientation of the CS planes are detectable? How well ordered are the structures?

2. Previous Phase Analyses of the System $TiO_2 + CrO_{1.5}$

By X-ray diffraction, ordered (121)$_r$ CS structures $Ti_{n-2}Cr_2O_{2n-1}$, with $n = 6$–9, were found to exist as single phases in samples quenched from 1573 to 1673°K. Diphasic mixtures were found at intermediate compositions (*4, 5*). If the oxygen/metal ratios were greater than $x = 17/9 = 1.889$ (22.2 mole% $CrO_{1.5}$) the patterns showed continuous line shifts, but no two-phase region was resolved until $x = 1.93$ (14% $CrO_{1.5}$), when the rutile

pattern appeared. Later work (6, 7) examined the temperature dependence of the phase relations. It was assumed that, at 1573°K, the region 22.2–14 mole % chromia also contained (121)$_r$ CS structures, with $n = 9$–17. At 8–14 % $n = 17$ (121)$_r$ apparently coexisted with rutile. The "rutile" phase was homogeneous in the region 0–8 % chromia (decreasing to 0–4 % at 1273°K). A slight increase in its a_r axis with increasing chromia content was attributed to Cr^{3+} in interstitial octahedral sites. It was presumed that at higher concentrations these aggregated to produce (121)$_r$ CS planes.

However, electron microscope studies (1) showed that $n = 8$ was the highest (121)$_r$ CS structure at 1573°K. As the chromia content decreased, the CS planes changed their orientation from (121)$_r$ to (253)$_r$ via the continuous sequence of high-index structures in the range $1.875 \leqslant x \leqslant 1.930$ (25–14 % chromia). The (253)$_r$ family occupied the range $1.930 \leqslant x \leqslant 1.955$ (14–9 % chromia) and, in the remaining range, the samples were apparently homogeneous "rutile." Later workers reported that the (121)$_r$ CS family extended up to $n = 11$ at 1573°K, before the CS plane swung around to (253)$_r$ (8). The discrepancy may be because they did not always use [1$\bar{1}$1]$_r$ zones to identify the CS plane (cf. below). The angle between (121)$_r$ and (hkl)$_r$ is less than 1 degree for $p/q > 18$, cf. Fig. 15 in Ref. (2). In the present study $n = 8$, 9, and 10 (121)$_r$ have been observed, but only in a sample cooled very slowly from 1573°K.

3. Experimental

Specimen Preparation

Koch–Light TiO_2 (99.5 %) contained a small proportion of anatase, which was transformed to rutile above 1273°K. Koch–Light Cr_2O_3 was of 5 N purity. These powders were weighed and mixed to give one gram samples, with overall compositions 0–25 mole % $CrO_{1.5}$. The mixtures were pressed at 1.3–1.5 tons psi to produce 2 × 15 mm pellets, which were then melted in a cold-hearth electric arc furnace (9). Homogeneity was ensured by melting the pellets from both sides. The buttons solidified and cooled to room temperature

in about 30 s. Fragments of these buttons were heated for three days at 1573°K, in platinum tubes (4 mm diam × 10–20 mm long) *sealed* to prevent loss of CrO_3 by evaporation. It was calculated that the tubes contained ample oxygen to ensure complete oxidation of the black (reduced) melted samples, as evidenced by the brown coloured products. In order to allow direct comparison of our results with those of Ref. (8) a further set of pellets was made and fragments sintered in sealed Pt tubes for 14 days at 1573°K. All samples were quenched by quickly removing the tubes from the furnace. A list of compositions and sample numbers is given in Table I.

Specimens were prepared for electron microscopy by crushing (1). The [1$\bar{1}$1]$_r$ zone diffraction patterns were obtained using a JEM-6A electron microscope. The lattice
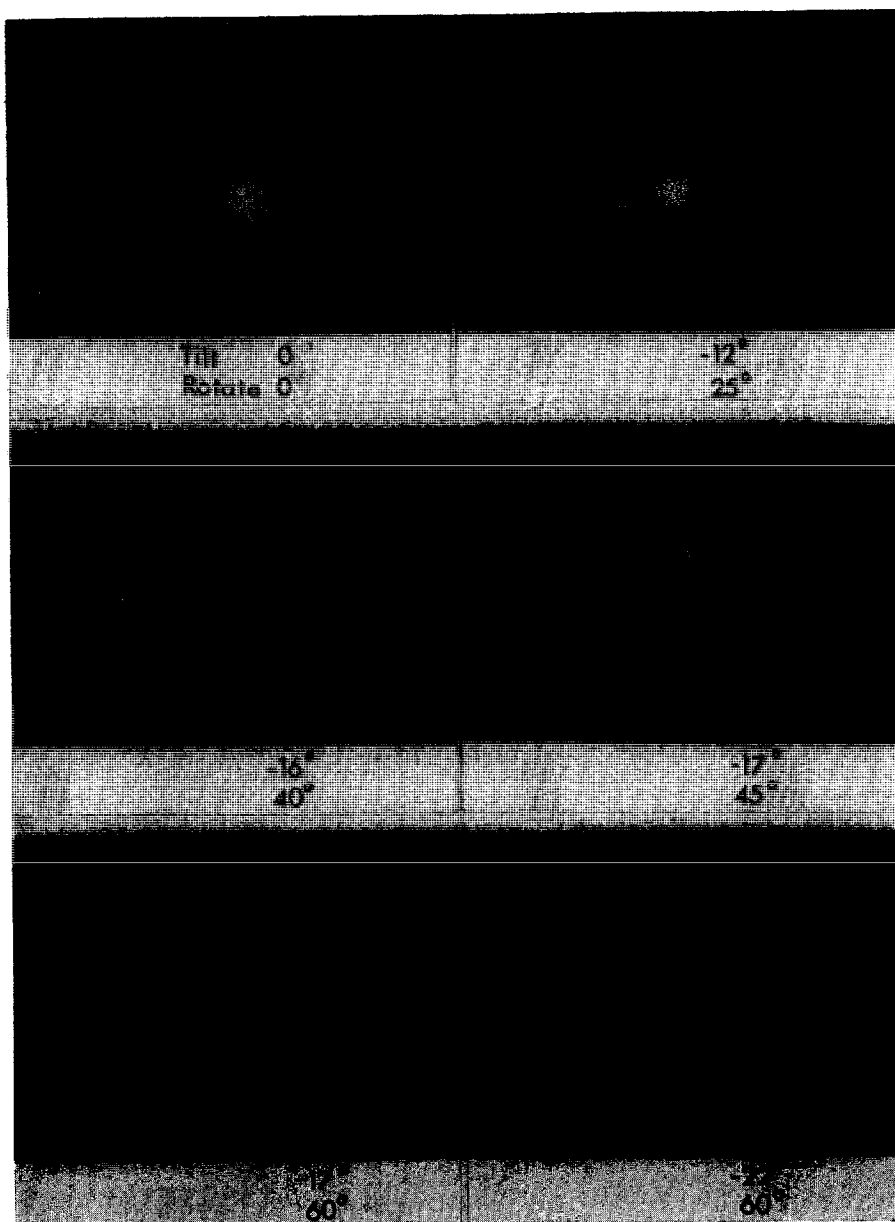
FIG. 1a–f. Sequence of diffraction patterns obtained while orienting a crystal so that the $[1\bar{1}1]_r$ zone axis is parallel to the incident beam, $p' = 3.7$, $D_{sp} = 1.62$ nm.

images were obtained with a Siemens Elmiskop 101. Goniometer stages and anticontamination devices were used.

Determining the CS Plane Indices, $(hkl)_r$

All of the observed CS planes $(hkl)_r = p \cdot (121)_r + q \cdot (011)_r$ lie in the $[1\bar{1}1]_r$ zone. To detect small orientation changes it is absolutely essential to orient the crystals so that the electron beam is exactly parallel to $[1\bar{1}1]_r$. Much time and effort may be required to obtain the correct orientation: a sequence of diffraction patterns illustrating the orienting process is given in Fig. 1.
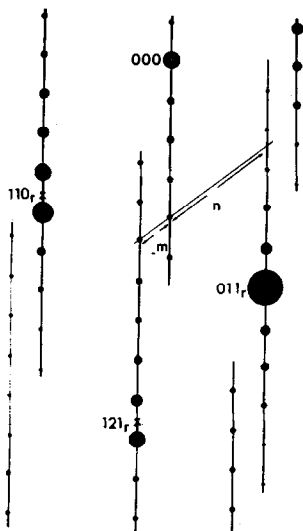
FIG. 2. Schematic drawing of $[1\bar{1}1]_r$ zone axis (projection of plate No. 23672), showing rutile reciprocal lattice positions, $p' = n/m = 3.26$.

Ordered $(hkl)_r$ CS planes give rows of superstructure spots normal to $(hkl)_r$. These intersect 121_r and 001_r q and p times, respectively (Fig. 2). In the rows, the spots are only visible close to the strong subcell reflections, and so it is not possible to count the intersections with 121_r and 011_r precisely: only the ratio $p/q = p'$ can be directly measured. This was done by projecting the negative (in a photographic enlarger), and tracing the rows of spots. The accuracy varies from 1 to 6% for $p' = 1$–10.

Measuring the CS Plane Spacing, D_{sp}

The ideal CS vector is $\frac{1}{2}[0\bar{1}1]_r$. Its component normal to $(011)_r$ is zero. This component is also zero for the measured vector $\frac{1}{2}[0, -0.90, 0.90]_r$ in $(132)_r$ CS structures (10). Measurements of X-ray powder patterns show that, in $Ti_{n-2}Cr_2O_{2n-1}$, d_{011_r} is altered by less than 1% (Table II). The 011_r reflection therefore

TABLE II

COMPARISON OF OBSERVED AND CALCULATED d_{011_r} VALUES FOR RUTILE
$(121)_r$ CS STRUCTURES

	$h\,k\,l^a$	Observed (d_{hkl}/nm)	Diff^b	%Diff
TiO_2	$0\,1\,1_r$	0.2487	—	—
$TiO_2 + 6$ mole% $CrO_{1.5}$	$0\,1\,1_r$	0.2488	0.001	0.04
Ti_nO_{2n-1}				
4	$1\,0\,4$	0.2524	0.0037	1.49
5	$1\,0\,2$	0.2515	0.0028	1.13
6	$1\,0\,4$	0.2512	0.0025	0.01
7	$1\,0\,2$	0.2508	0.0021	0.84
8^c	$1\,0\,4$	0.2506	0.0019	0.76
9^c	$1\,0\,2$	0.2503	0.0017	0.64
$Ti_{n-2}Cr_2O_{2n-1}$				
6	$1\,0\,4$	0.2500	0.0013	0.52
7	$1\,0\,2$	0.2500	0.0013	0.52
8	$1\,0\,4$	0.2499	0.0012	0.48
9	$1\,0\,2$	0.2498	0.0011	0.44

^{a} Indices of plane equivalent to $(011)_r$ in rutile transformed to M_nO_{2n-1} structure indices (Andersson and Jahnberg 1963).

^{b} Diff = observed $- d_{011_r}$.

^{c} The unit cells given in Andersson and Jahnberg (1963) are not consistent with their X-ray data, the correct unit cells for Ti_8O_{15} and Ti_9O_{17}, after refining their X-ray data, are:
$n = 8$; $a = 0.553$ nm, $b = 0.714$ nm, $c = 3.759$ nm, $\alpha = 99.16°$, $\beta = 128.37°$, $\gamma = 108.47°$. $n = 9$; $a = 0.552$ nm, $b = 0.714$ nm, $c = 2.226$ nm, $\alpha = 99.28°$, $\beta = 130.35°$, $\gamma = 108.48°$.
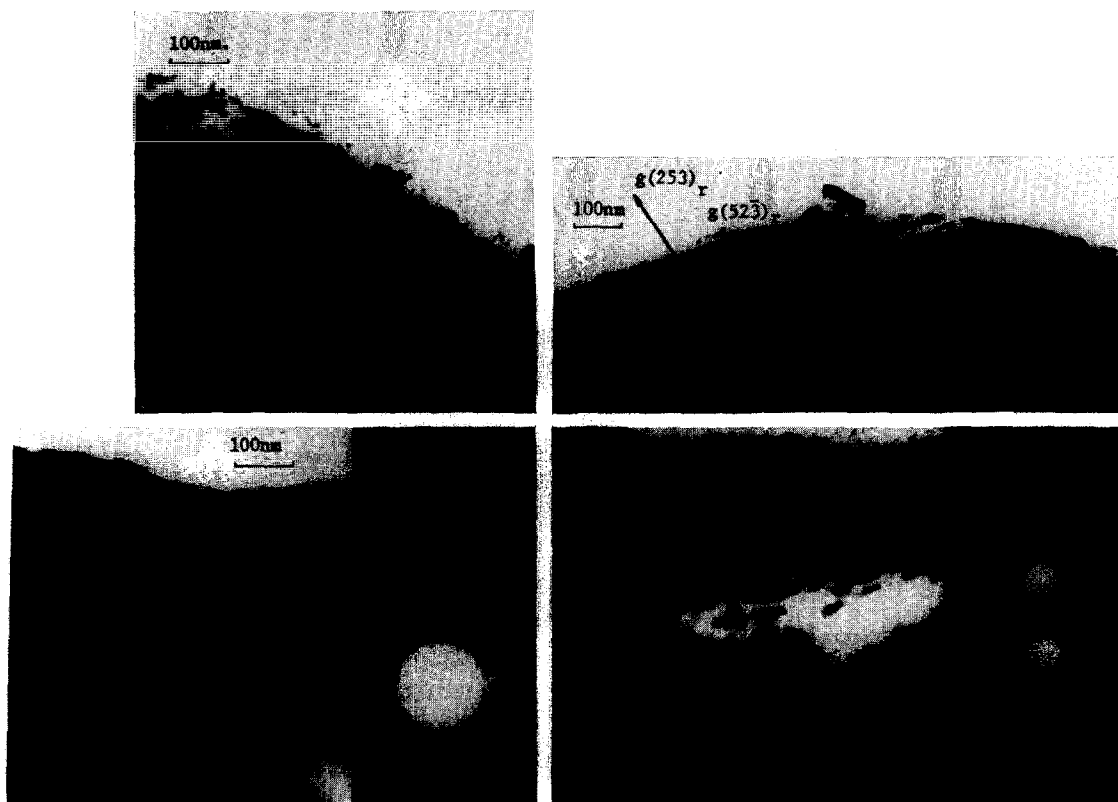
FIG. 3a. Mottled contrast in "rutile" flake, 6 mole% $CrO_{1.5}$, annealed at 1573°K. 3b. Line features approx parallel to $(253)_r$ and $(523)_r$ in a "rutile" matrix, 8 mole% $CrO_{1.5}$, annealed at 1573°K. 3c. Dislocations in contrast for $\bar{1}\bar{1}2_r$, sample 20. 3d. Area of 3c showing dislocations out of contrast for 110_r.

provides an internal standard in each $[1\bar{1}1]_r$ zone electron diffraction pattern. The camera constant and interplanar spacings, including D_{sp}, can therefore be measured with an accuracy of about 1%.

4. Observations

4.1. Up to 8 mole% $CrO_{1.5}$ ($2.000 \geqslant x \geqslant 1.960$)

(a) 1573°K

CS planes were not observed. The diffraction patterns were appropriate to rutile, and the spots were usually sharp, though sometimes diffuse scattering occurred. The "rutile" frequently showed mottled contrast (Fig. 3a) and, sometimes, short line features 10–25 nm long and approximately parallel to $\{253\}_r$ (Fig. 3b). Often there were $\{011\}_r$ faults, and an unusually high density of dislocations. Features in contrast for $\bar{1}\bar{1}2_r$ in Fig. 3c are out of contrast for 110_r in Fig. 3d. This is consistent with a Burgers vector $[001]_r$, whereas $\frac{1}{2}[0\bar{1}1]_r$ would give contrast for both these reflections. More complicated contrast was also observed, but no detailed interpretation attempted.

(b) 1273°K

Sample annealed for 40 days contained lamellae of $\{hkl\}_r$ CS structures in a rutile matrix. In Fig. 4a $(hkl)_r \simeq (385)_r = 3(121)_r + 2(011)_r$. The lamellae often zigzagged: Fig. 4c shows $(hkl)_r$ and $(hkl)_{r'}$. Within the lamellae the CS plane spacing is uniform $D_{sp} = 3.4$ nm, close to that measured at the centre of wide lamellae in reduced rutile (2). Under two-beam conditions the CS planes were in
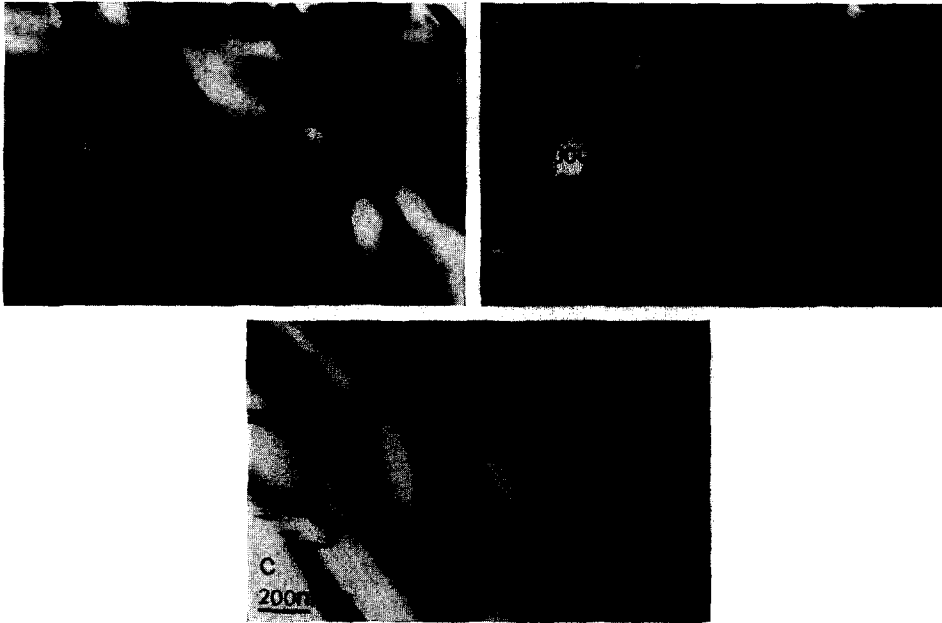
FIG. 4a. Lamellae of CS planes with indices close to $(385)_r$, 4 mole % $CrO_{1.5}$, annealed at 1273°K. 4b. Diffraction pattern of 4a, $[1\bar{1}1]_r$ zone, showing $p' \simeq 1.3$, $D_{sp} \simeq 3.4$ nm. 4c. Zigzag lamellae of $(132)_r$ and $(1\bar{3}2)_r$ CS structures in rutile matrix, 4 mole % $CrO_{1.5}$, annealed at 1273°K.

contrast for 002_r but extinguished for 011_r; weak contrast was observed for 120_r. These observations are consistent with the displacement vector $\frac{1}{2}\langle 0,-0.90,0.90\rangle_r$ found for $\{132\}_r$ faults (10). The vector $\frac{1}{10}[155]_r$, proposed in Ref. (11), is inconsistent with the observed 002_r contrast.

4.2. 8–25 mole % $CrO_{1.5}$; 1573°K

From 8 to 11%, ordered CS structures coexist with "rutile." Above 11% chromia, "rutile" is not observed.

(a) Electron Diffraction

As the chromia content increases, the $[1\bar{1}1]_r$ diffraction patterns show that the CS planes rotate from approx $(253)_r$, $p' \approx 2$, $D_{sp} \approx 2.2$ nm, to $(121)_r$, $p' = \infty$, $D_{sp} = 1.26$ nm. Each preparation yielded a small range in p' and D_{sp} values, but almost all the diffraction patterns were remarkably sharp (e.g., Fig. 5a, b). Table III lists the results (including p' and D_{sp}) for 9 $[1\bar{1}1]_r$ zone axis diffraction patterns for sample 39. Altogether 82 such patterns, from 17 different samples, were

obtained: 50 of them were measureably different. An expanded version of Table III, including the results for all the samples, is available on request. (Plots of measured p' and D_{sp} values, as a function of oxygen/metal ratio x, are given in Fig. 7a, b).

In the $(253)_r$ CS family only $n = 34–38$ were unequivocally established: higher n values occurred, up to $n = 47$, but the spots were not sharp enough for D_{sp} to be measured with an accuracy sufficient for n to be determined unambiguously. Earlier (1), we reported n values down to $28(253)_r$. It is now established that p' is slightly greater than 2.0 for "n" $\leqslant 33$.

Sample 24 was black, suggesting that some Ti^{3+} was present. It gave p' and D_{sp} values appropriate to a sample of lower oxygen/metal ratio (Table IV). Accordingly, it was reoxidized at 1073°K in air, and then reannealed at 1573°K. Its diffraction patterns were then quite consistent with its Cr/Ti ratio (sample 39 in Table III).

Sample 11 was slowly cooled from 1573°K to room temperature over a period of 15 hr (instead of being quenched). Its diffraction
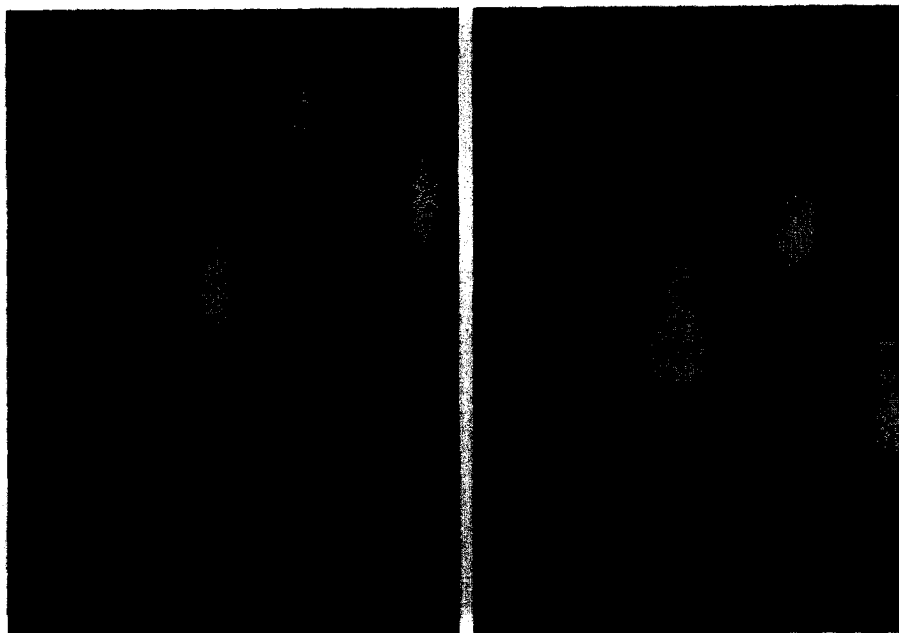
FIG. 5a, b. Indexed [1Ī1], zone axis diffraction patterns, showing $p' = 2.1$(a) and 3.7 (b).

patterns showed it to be a complex mixture of a wide variety of structures (Table V): p' varied from 3.2 through 25 to ∞, and D_{sp} between 1.27 and 1.91 nm. The phases $n = 8, 9, 10$ (121), were found in this sample.

(b) Lattice Images

The micrographs revealed surprisingly perfect textures: twinning was rare. A large number of lattice images was obtained, using the transmitted and several low order beams. Each one was remarkably regular, e.g., Fig. 6a (CS plane approx (9, 20, 11), Fig. 6b). A densitometer trace across Fig. 6a, shown in Fig. 6c, was measured with a travelling microscope. The mean spacing is 1.48 nm, and the standard deviation of 0.07 nm is just significant (Fig. 6d) compared with the precision

TABLE III

ANALYSIS OF [1Ī1], ZONE AXIS DIFFRACTION PATTERNS FROM SAMPLE
39, ANNEALED AT 1573°K (THE PREPARED OXYGEN/METAL RATIO WAS
$x = O/(Cr + Ti) = 1.9098$)

p' (measured)	p (assigned)	q	D_{sp} (measured)	n (fit)	x_{calc}	Δx
2.7(5)	11	4	1.65	137	1.920	−.010
2.3(6)	13	4	1.56	149	1.913	−.003
3.2(9)	13	4	1.53	146	1.911	−.001
3.4(8)	7	2	1.52	78	1.910	.000
3.6(0)	11	3	1.58	126	1.913	−.003
3.6(0)	11	3	1.53	124	1.910	.000
3.7(1)	11	3	1.47	117	1.906	.004
3.7(5)	15	4	1.47	159	1.906	.004
3.8(5)	27	7	1.42	278	1.902	.008

(a)   ‖   (e)
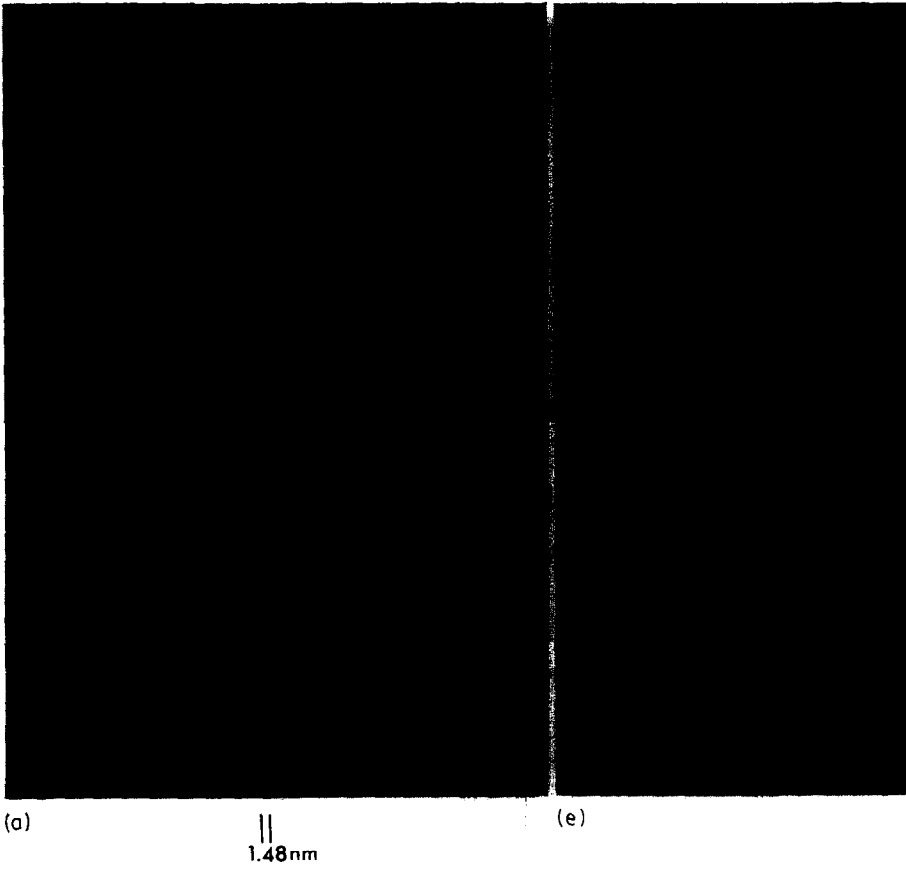   1.48nm

FIG. 6a. Lattice image of CS structure with $p' = 4.5$, $D_{sp} = 1.48$ nm.

FIG. 6c. Double exposure of 6a with an accurately square grid. Note small departure from linearity of fringes at A and B.

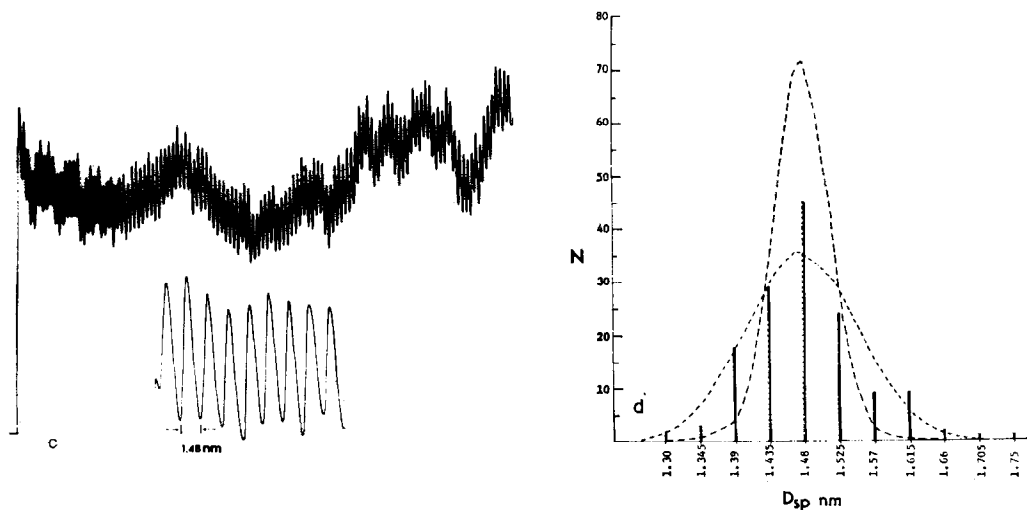FIG. 6b. [1$\bar{1}$1], zone axis diffraction pattern of 6a.

Fig. 6c. Densitometer trace across 6a, inset shows increased scale of part of trace.

Fig. 6d. Histogram showing distribution of fringe spacings of 6b. Curves show Gaussian distribution for the measurement accuracy (σ_{calc}) and for the measured standard deviation (σ_{meas}). (—— $\sigma = 0.035$. $D_{sp} = 1.48$ nm. ------ $\sigma = 0.07$. $D_{sp} = 1.48$ nm).

TABLE IV

DIFFRACTION RESULTS OF SAMPLE 24 (NOT FULLY REOXIDIZED)

p'	D_{sp} (nm)	Compositions using: O Cr + Ti 1	p' and D_{sp} 2	$\Delta x = 1-2$
7.0	1.36	1.9098	1.892	0.018
7.5	1.32	1.9098	1.888	0.022
7.8	1.32	1.9098	1.888	0.022
8.0	1.35	1.9098	1.890	0.020
8.0	1.37	1.9098	1.892	0.018
8.0	1.31	1.9098	1.887	0.023
8.2	1.35	1.9098	1.890	0.020
8.4	1.34	1.9098	1.889	0.021
9.4	1.37	1.9098	1.890	0.020
9.5	1.36	1.9098	1.890	0.020
12.5	1.35	1.9098	1.887	0.023
∞[a]	1.28	1.9098	1.875	0.035
∞[a]	1.28	1.9098	1.875	0.035
∞[a]	1.28	1.9098	1.875	0.035
∞[a]	1.29	1.9098	1.875	0.035
∞[a]	1.28	1.9098	1.875	0.035

[a] $n = 8$, $(121)_r$ CS structure.

of the measurements, 0.035 nm. (This ignores possible fringe displacements due to thickness variation or bending of the crystal. But these were minimized by carefully selecting an area with no apparent thickness or orientation changes.) About 10% of the measured spacings differ from the mean by $\geqslant 0.1$ nm.

The fringes appear to be straight and parallel but a closer inspection, by printing an accurately square grid over the fringes, reveals some very small orientation variations (A and B in Fig. 6e). The maximum variation of 0.5° appears to be spread over about 70 nm, without any obvious steps. Many other areas were studied in this way, with similar results. A great majority of the examined flakes appeared to be very well ordered, regardless of the orientation of the CS plane.

4.3 Melted Samples

Quenched melts from all preparations contained complex zigzag lamellae of faults. The more heavily doped specimens often showed complex microtwinning, presumably this is a strain relieving mechanism operating during the rapid nucleation/growth/quench period. Prolonged melting produced a wide

TABLE V

Diffraction Results from Sample 11, which was Cooled Slowly from 1573°K

| p' | D_{sp} (nm) | Compositions Using: | | |
		O Cr + Ti 1	p' & D_{sp} 2	$\Delta x = 1-2$
3.2	1.70	1.8897	1.924	−0.034
4.5	1.91	1.8897	1.925	−0.035
5.1₅	1.67	1.8897	1.913	−0.023
6.5₅	1.47	1.8897	1.900	−0.010
6.5₅	1.44	1.8897	1.899	−0.010
7.0	1.71	1.8897	1.913	−0.023
11	1.39	1.8897	1.891	−0.002
16	1.70	1.8897	1.908	−0.019
25	1.39	1.8897	1.888	+0.001
∞	1.27[a]	1.8897	1.875	+0.014
∞	1.27[a]	1.8897	1.875	+0.014
∞	+1.44[b]	1.8897	1.889	+0.000
∞	+Disorder			
∞	1.27[a]	1.8897	1.875	+0.014
∞	+1.44[b]	1.8897	1.889	+0.000
∞	+Disorder			
∞	1.27[a]	1.8897	1.875	+0.014
∞	+1.44[b]	1.8897	1.889	+0.000
∞	+Disorder			
∞	1.48[b]	1.8897	1.889	+0.000
∞	1.45[b]	1.8897	1.889	+0.000
∞	+1.62[c]	1.8897	1.900	−0.010
∞	1.44[b]	1.8897	1.889	+0.000
∞	+1.61[c]	1.8897	1.900	−0.010

[a] $n = 8$ (121)$_r$ CS structure.
[b] $n = 9$ (121)$_r$ CS structure.
[c] $n = 10$ (121)$_r$ CS structure.

range of behaviour; from isolated, widely spaced {132}$_r$ faults to CS structures down to $n = 6(121)_r$, with a large variety of p' and D_{sp} values. Similar textures have been observed previously in melted samples of rutile and reduced rutile (2). These results are presumably a consequence of loss of oxygen (and reduction of Ti^{4+} to Ti^{3+}) to the argon atmosphere at the high temperatures involved ($T_m \simeq$ 2150°K). These complex textures anneal out completely at 1573°K but remained after annealing at 1273°K, presumably because the rate was too low. This suggests that equilibration is extremely slow at this temperature.

5. Phase Identification

5.1. Indexing the Diffraction Patterns

A matrix relating the unit cells of the high-index CS structures with the rutile unit cell was derived. This enabled each diffraction pattern to be indexed (see e.g., Fig. 5a, b) and values of n, p, and q to be assigned (see Table III). A detailed discussion of the crystal structures, the derivation of the matrix and the indexing of the diffraction patterns is given elsewhere (12).

5.2. Calculating the Composition

The CS plane is

$$(hkl)_r = p \cdot (121)_r + q \cdot (011)_r$$
$$= q \cdot (p', 2p' + 1, p' + 1)_r.$$

The last term is a pseudo-Miller index, since p' may not be integral. Nevertheless, if we denote this plane by p', we have

$$d_{p'} = q \cdot d_{hkl_r}.$$

The spacing $d_{p'}$ depends only on the measured value of p' and is calculated using the pseudo-Miller indices.

The ideal displacement vector $\frac{1}{2}[0\bar{1}1]_r$ has a collapse component normal to $(hkl)_r$ which is the dot product:

$$g(hkl)_r \cdot \frac{1}{2}[0\bar{1}1]_r = g(p, 2p + q, p + q)_r \cdot \frac{1}{2}[0\bar{1}1]_r$$
$$= -p/2.$$

The CS plane spacing is therefore

$$D_{sp} = (n - p/2) \cdot d_{hkl_r}$$
$$= [n/q - p/2q] \cdot q \cdot d_{hkl}$$
$$= (n/q - p'/2) \cdot dp'.$$

Hence

$$n/q = D_{sp}/d_{p'} + p'/2.$$

Since the oxygen/metal ratio

$$x = (2n - p)/n$$
$$= 2 - p/n,$$

it follows that

$$x = 2 - q \cdot p'/n$$
$$= 2 - p'/(n/q)$$
$$= 2 - p'/(D_{sp}/d_{p'} + p'/2).$$

The error in this calculated x value, which
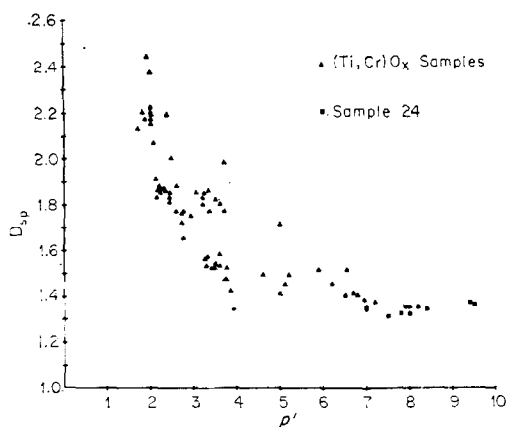
FIG. 7a. Plot of x_{calc} vs p'.

FIG. 7c. Plot of x_{calc} vs D_{sp}.

arises from uncertainties in p' and D_{sp} is $\geq 0.2\%$, i.e., $\pm \sim 0.004$. x was calculated from the measured D_{sp} and p' and calculated $d_{p'}$ values for each diffraction pattern. The prepared and calculated compositions are compared in Table III.

6. Discussion

6.1. Variation of Structure with Composition

(a) 0–8 mole % $CrO_{1.5}$

In one case the prepared composition was $x = 1.98$. The sample consisted of lamellae of $(253)_r$ faults, with $x = 1.97$, in a "rutile" matrix. If the latter were TiO_2 the lamellae would have occupied two-thirds of the volume. The observed proportion was much less,
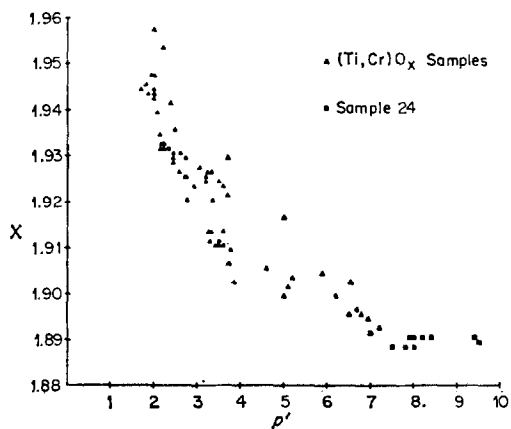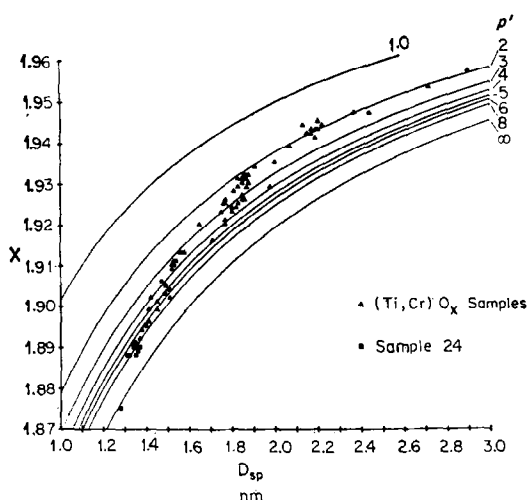

FIG. 7b. Plot of D_{sp} vs p'.

indicating that some of the chromium must have been accommodated by unresolved defects (<10 Å) in the "rutile" regions. These were presumably responsible for the "mottled" contrast, for the short line features approx parallel to $(253)_r$, and perhaps for the high density of dislocations in the matrix (Fig. 3). All these may contribute to the slight expansion of a_r with increasing chromium content revealed by X-ray diffraction (7).

The same sample, when annealed for 40 days at 1273°K contained lamellae of CS structures with $1 \leqslant p' \leqslant 2$ (Fig. 4a, b), but even then the composition of the "rutile" matrix was still less than $x = 2.000$. Clearly, a thorough study of the effect of temperature and annealing time on the precipitation of CS planes in the 0 to 8 mole % chromia range is necessary. It appears that some chromium can remain dispersed in "rutile." The critical concentration at which CS planes start to precipitate decreases with decreasing temperature and/or increasing time (see also Ref. (13)). Once they appear the CS planes show a strong tendency to aggregate and order.

(b) 8–25 mole % $CrO_{1.5}$

(i) *Electron diffraction.* Every crystal flake appeared to have its own, well ordered structure. Changes in stoichiometry are accommodated by both (i) cooperative reorientation of

the CS planes, i.e., varying p/q, and (ii) varying D_{sp}. At least 50 different structures were observed. For each preparation there is a narrow and, usually, significant spread of results; the prepared compositions agreed closely with those calculated from the diffraction patterns (Table III). At the lowest Cr contents p' was sometimes less than 2.

We have plotted x_{calc} vs p', D_{sp} vs p' and x_{calc} vs D_{sp} in Fig. 7a–c. The measurement errors $\delta(p')$ and $\delta(D_{sp})$ are 1–6% and 1%, respectively. It is clear that the relation between x_{calc}, D_{sp} and p' is not sharply defined. We believe that the main reason for the scatter is the very small differences between the partial molar free energies of the components in the various structures. The driving force to achieve equilibrium is exceedingly small. It is not possible to say whether both D_{sp} and p' change smoothly with x, or whether there are composition regions in which one of these is constant. Resolution of this point may be possible using very long anneals at constant temperature. There was no significant difference observed in the sharpness of the diffraction patterns of samples sintered for 14 days compared to those melted first, then annealed for 3 days.

The results from sample 11, which was slowly cooled over a period of 15 hr from 1573°K to room temperature, suggest that the end members of the swinging region are temperature dependent with the $(\bar{1}21)_r$ CS family extended to higher n values on cooling.

(ii) *Lattice images.* The area shown in Fig. 6a, approx $150 \times 150 \ \mu m^2$, shows no apparent spacing variations. Only 10% of the measured spacings were significantly above or below the mean value. From the diffraction pattern (Fig. 6b) $p' = 4.5 \pm 0.2$ and $D_{sp} = 1.48$ nm so that $x_{calc} = 1.905 \pm 0.006$. However, it must be noted that the difference in D_{sp} for adjacent n values is only 0.03 nm (0.3 Å) so that even though the lattice image has resolution of approx 5 Å it will be impossible to reveal mixtures of adjacent n values for such high-index CS structures. Similarly, there do not appear to be any gross variations in CS plane orientation (Fig. 6d). The maximum variation is 0.5° over a length of about 70 nm. If this is a real change in p', rather than elastic

bending of the crystal flake, then we must have $4 \leqslant p' \leqslant 4.6$, giving rise to a maximum composition variation $\Delta x = 0.002$. Thus while D_{sp}, p' and x have very narrow ranges we cannot assert that the structures must be perfectly ordered.

6.2. Comparison of the Results with Those of Previous Studies of $TiO_2 + CrO_{1.5}$

There are some differences between the present results and previous interpretations of the region 0–25 mole% $CrO_{1.5}$. Andersson et al. (4, 5) reported the existence of $n = 9(121)_r$ in samples prepared at 1573°K and cooled "fairly rapidly". We find $n = 8$ to be the highest $(121)_r$ CS structure in specimens quenched from the same temperature. At higher compositions $n = 8(121)_r$ coexisted with *high index CS* structures close to $n = 9$ in composition. At $x = 17/9$ $n = 8(121)_r$ was no longer present. Only high p' structures remained, though their X-ray powder diffraction patterns closely resemble that of $n = 9(121)_r$. We confirm that for $x > 17/9$, the X-ray powder patterns show continuous line shifts. These are readily understood in terms of the electron diffraction results: each rutile subcell line is split into a doublet or triplet and the magnitude of the splitting is directly dependent on D_{sp}, which varies continuously with composition. Each X-ray line may, in fact, be a superposition of several lines originating from different, but closely similar high-index structures (Philp (3), to be published).

Lee and Florke (6, 7) assumed that the $(121)_r$ family continued to $x = 1.93$, claiming that insufficient resolution prevented the identification of diphasic regions. This now appears to be incorrect.

From their electron diffraction analysis Gibb and Anderson (8) deduced that the highest $(121)_r$ member, at 1573°K, was $n = 11$. However, they used $[2\bar{1}0]_r$, $[\bar{1}01]_r$, and $[01\bar{2}]_r$ zone diffraction patterns to identify structures. For high index structures the angle $(hkl)_r \wedge (121)_r$ is small and in these zones the projected angle is almost exactly parallel to $(121)_r$. Thus the superlattice rows could well have appeared to be parallel to $(121)_r$. (However $n = 11(121)_r$ has $D_{sp} = 18.0$ Å. At this value we

find $p' = 3$, which is quite low: the angle $(121)_r$ $\wedge (374)_r = 5°$, which is not small!) We emphasize the absolute necessity to obtain symmetrically excited $[1\bar{1}1]_r$ zones (see Fig. 1) for accurate identification of $(hkl)_r$.

6.3. Comparison of the Results with Those from Other Rutile CS Systems

The diffraction patterns from the (Ti, Cr)O_x samples prepared at 1573°K were markedly sharper than those from TiO$_x$ (in the swinging CS plane region) prepared at 1273°K. Lattice images from the latter show a discernible range of p' values *within* each crystal flake (2). A more recent study of TiO$_x$, prepared by quenching from 1473°K (Bursill, unpublished) yielded very sharp diffraction patterns, indistinguishable in quality from those of (Ti,Cr)O_x. It therefore seems likely that the earlier problem was simply a kinetic one.

In the (Ti,Cr)O_x system at 1573°K, the swinging region is from $n = 8(121)_r$–$n = 38(253)_r$; i.e., $1.875 \leqslant x \leqslant 1.947$, $1.30 \leqslant D_{sp} \lesssim 2.4$ nm. In the TiO$_x$ system the temperature dependent limits are: at 1273°K; $n = 9(121)_r$–$n = 16(132)_r$; i.e., $1.889 \leqslant x \leqslant 1.938$, $1.46 \leqslant D_{sp} \leqslant 1.62$ nm: at 1473°K; $n = 8(121)_r$–$n = 20(132)_r$, i.e., $1.875 \leqslant x \leqslant 1.950$, $1.30 \leqslant D_{sp} \leqslant 2.00$ nm.

Hence the composition range of the high-index CS structures increases with increasing temperature. The lower boundary moves to lower compositions at higher temperatures. Similar behaviour has been observed in the (Ti,Fe)O_x system (13) although, in this case, the changes are more dramatic because they occur over a much small composition/temperature range, e.g., at 1450°K; $n = 16(121)_r$–$n = 75(253)_r$; i.e., $1.934 \leqslant x \leqslant 1.956$, $2.6 \leqslant D_{sp} \leqslant 4.8$ nm. At 1573°K lamellae of $n = 30(121)_r$ coexist with isolated $(132)_r$ faults, i.e., at low temperatutes the $(121)_r$ and $(132)_r$ segments have completely unmixed. The results for sample 11 above suggest that a similar situation may obtain in the (Ti,Cr)O_x system. Clearly, a thorough study as a function of temperature is necessary.

We have not been able to obtain from our electron microscopic studies of (Ti^{4+},Ti^{3+})O_x, (Ti^{4+},Cr^{3+})O_x or (Ti^{4+},Fe^{3+}/Fe^{2+})O_x any unambiguous evidence that the M^{3+} ions are located in the CS planes. Marezio et al. (14) showed that for Ti$_4$O$_7$($n = 4(121)_r$)Ti^{3+} is not localized at face-shared octahedral sites in the CS plane, but is distributed over all the metal atoms. This can easily occur by electron switching, Ti^{4+} + e$^-$ = Ti^{3+}, in the binary system. This is not so for the ternary systems. The observations on slightly doped rutile (0–8 mole% CrO$_{1.5}$ or FeO$_{1.5}$) (see above and (13)) show that it is M^{3+} diffusion which controls the kinetics of CS plane production and strongly suggests that the M^{3+} ions are precipitated at the CS planes. Single crystal structure determinations of some ternary CS structures are required to settle this point.

7. Conclusion

We have confirmed in considerable detail that the region rutile plus 8–23 mole% chromia, at 1573°K, exhibits a continuous series of highly ordered structures with no diphasic regions. For comparison with thermodynamic measurements and theories it seems to us that this region should be regarded as *one phase*, consisting of an extremely large number of closely related structures, rather than *multiphase*, with a large number of slightly different structures. This is consistent with standard definitions of a phase, e.g., "a homogeneous system, whose properties are the same in all parts, or at least which *vary continuously from point to point*; that is, there are no apparent surfaces of discontinuity" (15). Our studies reveal a novel phase whose homogeneity is retained, but whose structure varies continuously, as a function of composition ("phase" is not necessarily synonymous with "structure"). Lattice images provide the most direct criterion or measure of homogeneity. Our crystals were homogeneous to a resolution considerably better than 15 Å. Within experimental error there is an essentially continuous variation of CS plane spacing and orientation with composition. Detailed discussion of high-index CS plane structures, possible alternative structures, and possible subtle fluctuations in structure, not revealed in the present study, will be published elsewhere.

Analogous continuous structural variations and diffraction phenomena no doubt occur in numerous other systems. It remains to be seen whether these will be as amenable to study as they have been in this system.

Acknowledgments

References

1. L. A. BURSILL, B. G. HYDE, AND D. K. PHILP, Phil. Mag. 23, 1501 (1971).

2. L. A. BURSILL AND B. G. HYDE, Progr. Solid State Chem. 7, 177 (1972).

3. D. K. PHILP, Ph.D. Thesis, University of Western Australia, 1972.

4. S. ANDERSSON, A. SUNDHOLM, AND A. MAGNÉLI, Acta Chem. Scand. 13, 989 (1959).

5. S. ANDERSSON AND L. JAHNBERG, Arkiv Kemi 21, 413 (1963).

6. C. W. LEE, Ber. Deut. Keram. Ges. 47, 169 (1970).

7. O. W. FLORKE AND C. W. LEE, J. Solid State Chem. 1, 445 (1970).

8. R. M. GIBB AND J. S. ANDERSON, J. Solid State Chem. 4, 379 (1972).

9. T. B. REED, Mater. Res. Bull. 2, 349 (1967).

10. L. A. BURSILL AND B. G. HYDE, Proc. Roy. Soc. (London) Ser. A 320, 147 (1970).

11. J. VAN LANDUYT, R. DE RIDDER, R. GEVERS, AND S. AMELINCKX, Mater. Res. Bull. 5, 353 (1970).

12. D. K. PHILP AND L. A. BURSILL (1973), Acta Cryst. (in press).

13. L. A. BURSILL, J. Solid State Chem. 9, (1974).

14. M. MAREZIO, D. B. McWHAN, P. D. DERNIER AND J. P. REMEIKA, J. Solid State Chem. 6, 213 (1973).

15. G. N. LEWIS, M. RANDALL, K. S. PITZER AND L. BREWER, "Thermodynamics," 2nd Ed. p. 7. McGraw-Hill, New York 1961).